Coastal Engineering 99 (2015) 167–175

Contents lists available at ScienceDirect

Coastal Engineering

journal homepage: www.elsevier.com/locate/coastaleng

# Observations and modeling of alongshore variability in dune erosion at Egmond aan Zee, the Netherlands

R.C. de Winter *, F. Gongriep, B.G. Ruessink

*Department of Physical Geography, Faculty of Geosciences, Institute for Marine and Atmospheric Research, Utrecht University, P.O. Box 80.115, 3508 TC Utrecht, Netherlands*

ARTICLE INFO

*Article history:*
Received 5 June 2014
Received in revised form 27 January 2015
Accepted 9 February 2015
Available online 30 March 2015

*Keywords:*
Dune erosion
XBeach
Alongshore variation
Observations
Modeling

ABSTRACT

Dunes can erode within a few hours when exposed to high storm surge levels and large waves. If the dunes are the primary defense, such as in the Netherlands, this could result in flooding of the hinterland when dunes breach. Models are often used to analyze how dunes will respond to extreme conditions, but they can also be applied to study milder events, and with that gain more insight in the processes of dune erosion. There is, however, growing demand for validating existing models under field conditions. Here, we calibrate the XBeach dune erosion model with pre- and post-storm topography measurements of the dune-erosion event in January 2012 at Egmond aan Zee, The Netherlands. Furthermore, hydrodynamical data of the intertidal zone along a cross-shore transect in the same area collected 3 months prior to the storm event are used to hydrodynamically calibrate and validate XBeach. During the January 2012 storm the dune erosion was variable alongshore, from the erosion of embryo dunes, the forming of a dune scarp to considerable slumping of the entire dune face. This caused the erosion volume $V$ to range from 5 to 40 $m^3/m$. The calibrated model reproduces the alongshore variability in $V$ with reasonable accuracy. Additional simulations show that the alongshore variation in $V$ is due to variability on the initial dune topography (primarily steepness), and that variability in beach and nearshore bathymetry was of secondary importance.



## 1. Introduction

Dunes are part of natural, sandy wave-dominated coastal systems. They can erode severely in a matter of hours when exposed to high storm surge levels and large waves, while they grow slowly during calm conditions as a result of aeolian processes. For coastal safety purposes it is important to understand the processes underlying the rapid erosion events, as dunes are often the primary barrier against marine flooding. This is especially relevant for cases where the hinterland is densely populated and low-lying, as in the Netherlands. To analyze and understand the processes that cause dune erosion, flume experiments and models are often used, because with these two methods controlled and prescribed storm conditions can be studied. There is a growing demand for validating existing models under field conditions, given potential scaling issues with laboratory findings (Van Rijn et al., 2011) and the assessment of climate-change effects on coastal evolution.

Over the years, a wide variety of dune-erosion models have been developed, differing in complexity and hence (operational) applicability. Based primarily on laboratory experiments and only limited field data, empirical dune-erosion models (e.g. Van de Graaff, 1977; Vellinga, 1982; Van Gent et al., 2008) predict the final (equilibrium) dune-erosion profile with the erosion volume depending on, among other factors, wave height and period, surge level and grain size. The computational ease of these one-dimensional (i.e., cross-shore profile) models allows them to be embedded in a probabilistic setting (e.g. Den Heijer et al., 2012) and to be applied in operational coastal safety assessments, such as in the Netherlands. However, the underlying assumption of alongshore uniformity in waves and morphology is rarely met in nature. Furthermore, the equilibrium models are strictly valid for the range of conditions for which they were derived. This may be problematic for quantifying climate-change induced changes in future dune erosion. For example, the current operational equilibrium dune-erosion model DUROS+ (Van Gent et al., 2008) assumes shore-normal waves only and can thus not be used to study potential changes in the angle of wave incidence.

To remedy the shortcomings of equilibrium models, other, more complicated dune-erosion models have been developed. These models base dune erosion on wave impacts (Kriebel & Dean, 1993; Larson et al., 2004), the hydrology within the eroding dune (Palmsten & Holman, 2011), or the hydrodynamics and sand transport in front of the eroding dune (Van Rijn et al., 2011; Roelvink et al., 2009; Kobayashi et al., 2009). Within the latter process-based category, especially the model XBeach (Roelvink et al., 2009) has become widely used in coastal-impact studies (e.g. McCall et al., 2010; Splinter & Palmsten, 2012; Corbella & Stretch, 2012; Callaghan et al., 2013; Splinter et al., 2014; Long et al., 2014; Stockdon et al., 2014). A large benefit of more process-based models, including XBeach, is that they can be run in

* Corresponding author. Tel.: +31 30 2533275.
*E-mail address:* r.c.dewinter@uu.nl (R.C. de Winter).

http://dx.doi.org/10.1016/j.coastaleng.2015.02.005
0378-3839/

two-dimensional mode (i.e. area) and therefore can handle alongshore variability in topography. In addition, free model parameters can be adjusted to minimize data-model mismatch.

Despite XBeach's increased use, limited field-based studies have been executed to calibrate and validate XBeach's parameter settings in its hydrodynamical and morphological modules. McCall et al. (2010) concluded that XBeach is capable of producing morphological features common to overwash based on a study for Santa Rosa Island after hurricane Ivan. For the area where post-storm lidar data was available they obtained a mean model skill of 0.72. Other XBeach modeling studies related to field conditions include Splinter & Palmsten (2012), Corbella & Stretch (2012), Callaghan et al. (2013) and Splinter et al. (2014). They all analyzed erosion events for individual cross-shore profiles, not taking advantage of area-mode capability and exploring any alongshore variability in dune erosion. Van Thiel De Vries et al. (2011) and Den Heijer (2013) used XBeach in area mode to suggest that alongshore erosion differences are largely determined by the upper part of the profile, for example, dune height. Differences in alongshore dune erosion can also be due to alongshore variability in offshore and nearshore bathymetry. Claudino-Sales et al. (2008) and Houser et al. (2008) suggested that the alongshore erosion differences at Santa Rosa Island after hurricane Ivan were mainly caused by offshore bathymetry differences (e.g. transverse ridges on the inner shelf) that locally focus wave energy and therefore cause alongshore variations in dune erosion. Similar findings have also been reported by Bender & Dean (2003), Schupp et al. (2006) and (Galal & Takewaka (2011). Thornton et al. (2007) related localized erosional hot-spots to the presence of persistent rip channels. It is important to realize that most field studies were largely descriptive, while most model studies were exploratory or lacked sufficient data for hydrodynamical and morphological calibration.

This paper has two main objectives. The first objective is to calibrate the hydrodynamical and morphodynamical parameter setting of XBeach for a field case. Our morphological data cover a dune-erosion event in January 2012 at Egmond aan Zee, the Netherlands. Eventhough the coast is uninterrupted and locally uniform to the eye, dune erosion was alongshore variable, from the erosion of embryo dunes to considerable slumping of almost the entire ~25 m high dune face. During a fieldcampaign in the autumn of 2011 at Egmond aan Zee, we also obtained hydrodynamical data on an intertidal cross-shore profile under storm conditions. This data set allows us to hydrodynamically calibrate and validate XBeach (Section 2.3). With the calibrated free parameters in the hydrodynamical module, we then calibrate XBeach on observed dune erosion data (Section 3.2). The second objective of this paper is to use XBeach in exploring the underlying causes for the differences in alongshore erosion volumes at these relatively high dunes under storm surge (Section 3.3).

## 2. Methodology

### 2.1. Study site

Alongshore variability in dune erosion was investigated with topographic surveys from Egmond aan Zee, the Netherlands (hereafter referred to as Egmond). Egmond, located along the approximately 120-km long uninterrupted Holland coast, is a wave-dominated beach that comprises three subtidal sandbars (e.g., Pape et al., 2010), a slip-face ridge (e.g., Masselink et al., 2006) on the fairly flat ($\approx 1:30$) intertidal beach, and an approximately 25-m high foredune that is largely covered in European marram grass (*Ammophila arenaria*). The medium size $D_{50}$ of the quartz sand is ~0.3 mm. The site is approximately north–south oriented and is predominantly exposed to sea waves generated on the North Sea. Recordings of a near-by directional wave buoy, located in about 26-m depth, show an annual average significant wave height and peak period of $H_s = 1.3$ m and $T_p = 5.9$ s, respectively, between 1999 and 2011. Particularly during storms with north-westerly winds, $H_s$ can increase to over 7 m, with a corresponding $T_p$ of about 12 s. The tide is micro-tidal and the semi-diurnal spring tidal range is just below 2 m. These numbers are based on recordings of two tidal stations (Petten Zuid and IJmuiden Buitenhaven), located about 15 km north and south of Egmond, respectively. The tide level at Egmond is, following Van Enckevort & Ruessink (2001), taken as the average of both sites. Storm surges can raise the water level by typically 0.5 to 1.5 m, but surges that are sufficiently high for storm waves to reach the foredune are rare. Embryo dunes can develop on the upper beach in front of the foredune during years without any noteworthy storms and associated surges (Fig. 1a–d). Egmond has been the focus of considerable earlier nearshore investigations, in part because of the approximately 50 m high video (Argus) tower installed here in 1998 (Van Enckevort & Ruessink, 2001).

### 2.2. Data collection

The storm we focus on here took place from January 3 to 6, 2012, when the offshore $H_s$ was persistently above 2 m and peaked just below 6 m in the night from January 5 to 6 (Fig. 2a). The offshore $T_p$ was high throughout the entire storm ($\approx 9$ s) and peaked at 11.5 s when $H_s$ was highest (Fig. 2a). The waves were always obliquely incident, initially from the south–west (negative wave angles $\theta$ in Fig. 2b), then veered to the north–west (positive $\theta$) just before the peak of the storm. The offshore water level reached maximum values of 2 m above mean sea level (MSL, Fig. 2c), implying an approximate surge height close to 1 m. The available Argus imagery demonstrates that the dunes were eroded primarily during the two high tides on January 5.

#### 2.2.1. Topographic surveys

The pre-storm survey was performed as part of a nearshore field campaign (see De Bakker et al., 2014) on October 14, 2011 using a RIEGL VZ-400 3D terrestrial laser scanner (TLS). The TLS was deployed from a tripod with the instrument about 2 m above beach level at two positions and one from the top of the foredune. At each position the TLS collected data through 360° in the horizontal plane and 100° in the vertical at distances up to 100 m, with a rate of 122,000 points/s and an angle resolution of 0.04° in the horizontal and vertical. Four retro-reflective cylinders were placed within view of the TLS to allow referencing the scan data to an alongshore oriented local co-ordinate scheme with its origin near the video tower; positive $x$ is directed onshore, positive $y$ is alongshore to the south. Each scan was manually filtered to remove non-surface items, such as people, cars and waves, and then averaged into a digital terrain model with a 0.2 (cross-shore) × 0.5 m (alongshore) resolution. All heights are relative to Dutch Ordnance Datum (NAP), which is approximately mean sea level (MSL).

The post-storm survey was conducted with the same TLS on January 10, 2012. Six scans with the same angle settings and with the TLS spaced 150 m in the alongshore were performed and subsequently processed identically as the pre-storm scans. As the pre-storm survey was less extensive in the alongshore than the post-storm survey, we can compute topographic change for an approximate 500-m long stretch of coast north of the video tower only ($y = -500$ m to 25 m). It is likely that the intertidal morphology just before the storm was somewhat different from the pre-storm survey because of cross-shore and alongshore intertidal sandbar migration (e.g., Quartel et al., 2007). The available video images show, however, no changes to the upper beach and the foredune between the pre-storm survey and early January 2012 before the storm. The post-storm data in the $y = -500$ to $-350$ m region are incomplete because the 10–15 m wide region between the remnants of the embryo dune field and the dune face was in the TLS shadow (i.e., could not be illuminated by the TLS; see Fig. 1e). This was not the case during the pre-storm survey as one of the 3 scan positions was on the top of the foredune. Embryonic dunes were not present elsewhere.

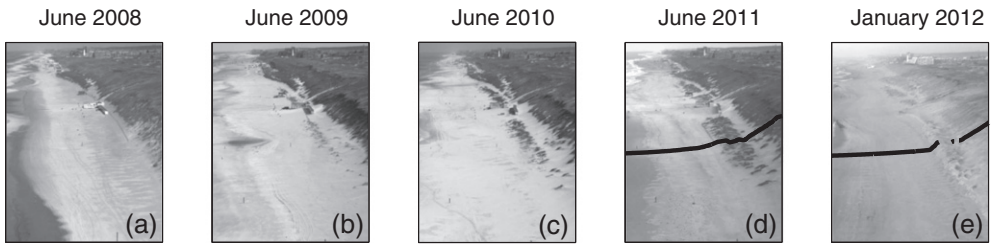


**Fig. 1.** Generation and growth of an embryo dune field (a–d) at Egmond, followed by its near-complete erosion (e) during the storm in early January 2012 investigated in this paper. The initial generation of the embryo dune field may have been triggered by a fence extending from the beach restaurant toward the camera, clearly visible in 2008. Annual surveys of cross-shore profiles through the growing dune field show an increase in sand volume of about 33 $m^3$/m between April 2008 and January 2012, corresponding to an annual aeolian sand input of about 11 $m^3$/m/year. All images were captured by camera 1 of the Argus video tower at Egmond. The black lines in d) and e) represent the measured pre- and post-storm profile at $y = -500$ m, see Section 2.2, the southern end of our study site.

*2.2.2. Hydrodynamics*

Near-bed pressure was collected at Egmond at 12 cross-shore locations during a six-week period in autumn 2011, see De Bakker et al. (2014) for details. All pressure data were converted to sea-surface elevation using linear theory, and were processed into significant short-wave (0.05–1 Hz) and infragravity (0.005–0.05 Hz) wave heights, denoted $H_{ss}$ and $H_{inf}$, respectively, using standard spectral techniques. The bed profile along the instrument array, which spanned from the spring-low to spring-high tide level, was measured several times per week using a RTK-Global Positioning System. The bed profile between the low-tide level and 15-m water depth, roughly 1750 m from the low-tide line, was surveyed with a ship in early November 2011.

## 2.3. Model

*2.3.1. General description*

We used the 2D-horizontal XBeach model (version V19-easter) to predict the coupled nearshore hydrodynamics and sand transport on the wave group scale, and the resulting bed level change, to examine the dune erosion during the January 2012 storm described in Section 2.2. XBeach includes a non-stationary wave driver with directional spreading to resolve infragravity-wave motions, which are important to beach and dune erosion (e.g. Russell, 1993; Thiel et al., 2008). XBeach has previously been documented extensively (e.g. Roelvink et al., 2009) and we therefore forgo a full model description here.

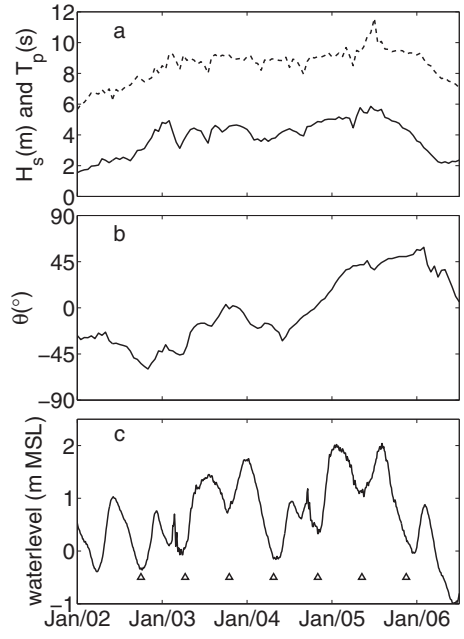


**Fig. 2.** Offshore hydrodynamical conditions between 3 and 7 January 2012, a. solid line: significant wave height $H_s$ (m), dotted line: peak period $T_p$ (s), b. wave angle $\theta$ (°) with respect to shore normal, c. water level (m) with respect to mean sea level (MSL), Δ times of bed level output, see Section 3.2.

*2.3.2. Hydrodynamic calibration and validation*

Before we used XBeach to simulate the January 2012 dune-erosion event, we calibrated and validated XBeach on the wave-height data collected in autumn 2011. For this, XBeach was run only in hydrodynamic mode, without sand transport and bed update computations. From the available data, we selected eight 2-hour long data blocks centered around high tide from all sensors. For these eight selected periods, offshore $H_s$ was between 2.5 and 3.8 m, $T_p$ between 6.2 and 7.8 s, and $\theta$ between approximately $-30°$ to $+50°$. We specifically chose blocks around high tide because of the approximately stationary in wave heights and water levels during that time period. The measured $H_{ss}$ varied between about 0.3 and 1.1 m and declined strongly toward the shore, while the measured $H_{inf}$ varied between 0.25 and 0.45 m and was approximately cross-shore constant, see also De Bakker et al. (2014).

The model was set-up in 2D (area) mode with alongshore uniform bathymetry; for the intertidal zone, the profile surveyed closest in time from the selected high tide was taken, while for the subtidal zone up to a depth of 15 m the ship survey of early November was used. The offshore wave conditions were used to create a Jonswap spectrum with an imposed directional spreading of 15°. The directional short-wave field was then used by XBeach to create the frequency-directional infragravity wave spectrum at the offshore boundary. Because in 1D (profile) mode XBeach prescribes the cross-shore component of the full infragravity field only (Van Dongeren, personal communication), we specifically set-up the model in 2D area mode to have the full infragravity field as input. The cross-shore × alongshore dimension of the grid amounted to 1764 × 1120 m, with a cross-shore and alongshore grid resolution of $\Delta x = 1$ m and $\Delta y = 5$ m in the shoreward center of the domain. Toward the seaward and lateral boundaries, $\Delta x$ and $\Delta y$ increased to 7.6 and 20 m, respectively. After a spin-up time of ~16 min, the simulation was run for 2 h and hydrodynamic data was stored every second.

For one of the eight tides ($H_s = 2.6$ m, $T_p = 6.2$ m, $\theta = -32°$), we ran simulations in which we varied the two free parameters in XBeach's wave module, $\gamma$ and $n$, see also Roelvink (1993) and Roelvink et al. (2009). Parameter $\gamma$ was varied between 0.4 and 0.9, and parameter $n$ between 5 and 20. Data-model error was quantified with the root–mean–square error $\varepsilon_{rms}$, computed separately for the short and infragravity waves. The simulations, reported fully in Gongriep (2013), illustrated that the short wave $\varepsilon_{rms}$ depends largely on $\gamma$ with, except for $\gamma = 0.4$, the lowest values for $n = 5$. Such low $n$, however, caused XBeach to under predict $H_{inf}$ considerably, implying that the grouped structure of the incident short waves is suppressed unrealistically. Because of the importance of infragravity waves to dune erosion, we considered $n = 10$ and $\gamma = 0.55$ as a compromise in simultaneously

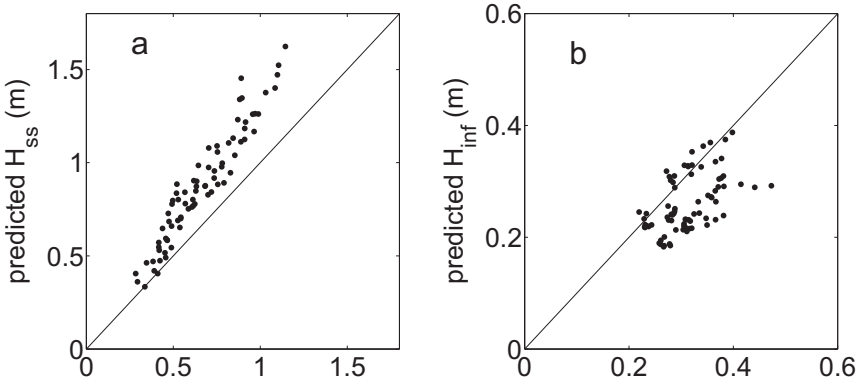


**Fig. 3.** a. Predicted significant wave height of sea swell $H_{ss}$ (m) versus observed $H_{ss}$ (m); b. same for significant wave height of infragravity waves $H_{inf}$ (m).

having adequate $H_{ss}$ and $H_{inf}$ predictions. This corresponds to the default values of $n$ and $\gamma$, which are advised to use when no hydrodynamical calibration is possible. These settings were then applied to the other seven tides. Predicted $H_{ss}$ and $H_{inf}$ versus measured values are presented for these seven tides in Fig. 3. The corresponding $\varepsilon_{rms}$ for the short and infragravity waves amounted to 0.086 and 0.043 m, respectively. In more detail, it can be seen that all $H_{ss}$ were overpredicted, especially the higher values: the slope of the best-fit line between measured and predicted $H_{ss}$ amounts to 1.4. As mentioned, reducing $n$ or $\gamma$ would improve the $H_{ss}$ predictions, but this would go at the expense of $H_{inf}$. The mismatch between observed and predicted $H_{ss}$ may also be due to uncertainties in the depth profile seaward of the intertidal zone, as it was surveyed some 3 weeks after the selected tides. We adopted $n = 10$ and $\gamma = 0.55$ in all dune-erosion simulations.

## 3. Dune erosion

### 3.1. Observations

The pre-storm dune topography was measured 3 months prior to the storm and could have been altered before the storm. Based on Argus-video images, we assume, however, the dune profile to have largely remained the same. The maximum offshore surge level during the storm was 2 m, which inundated the beach. Dune erosion in the approximately 500 m long coastal stretch for which we have a pre-storm and post-storm survey varied strongly alongshore. In the northernmost part ($y = -500$ to $-350$ m) an embryo dune field was largely eroded (Fig. 1d–e), while in the center ($y = -350$ to $-200$ m) a scarp had formed (Fig. 4a). The height of this scarp grew in the southward direction from approximately 1 m to over 5 m. Further to the south ($y = -200$ to 25 m), most of the dune face had fallen down in a series of slumps (Fig. 4b).

The three different erosion zones are also visible in the topographic difference map (Fig. 5a; note that this map focuses on the upper beach and foredune only). The eroded embryo dune field can be seen as an approximately 5–10 m wide area with patchy erosion patterns, with height changes between 1 and 3 m. As explained in Section 2.2, part of the data behind the remains of the embryo dunes are missing, resulting in blanks in Fig. 5a. The scarp region is the relatively narrow erosion strip, with height changes generally less than 2 m. The slumps and their presence over much of the dune face are visible as erosion lobes with height changes over 4 m and an overall cross-shore widening of the erosion area to some 15 m, respectively. It is also here that the maximum height to which the erosion extended is largest ($\approx$ 15 m above MSL, see Fig. 5b). All cross-shore post-storm profile lines contained an abrupt change in slope near 2.6 to 2.8 m above MSL, marking the new transition of the beach to the dune face (Fig. 6). The height of this transition is thus some 1 m higher than the maximum offshore water level,


**Fig. 4.** a. Dune scarp, representative of $y \approx -350$ m to $-250$ m b. dune scarp on the left changing into mass movement (slumping) toward the right ($y > -200$ m).

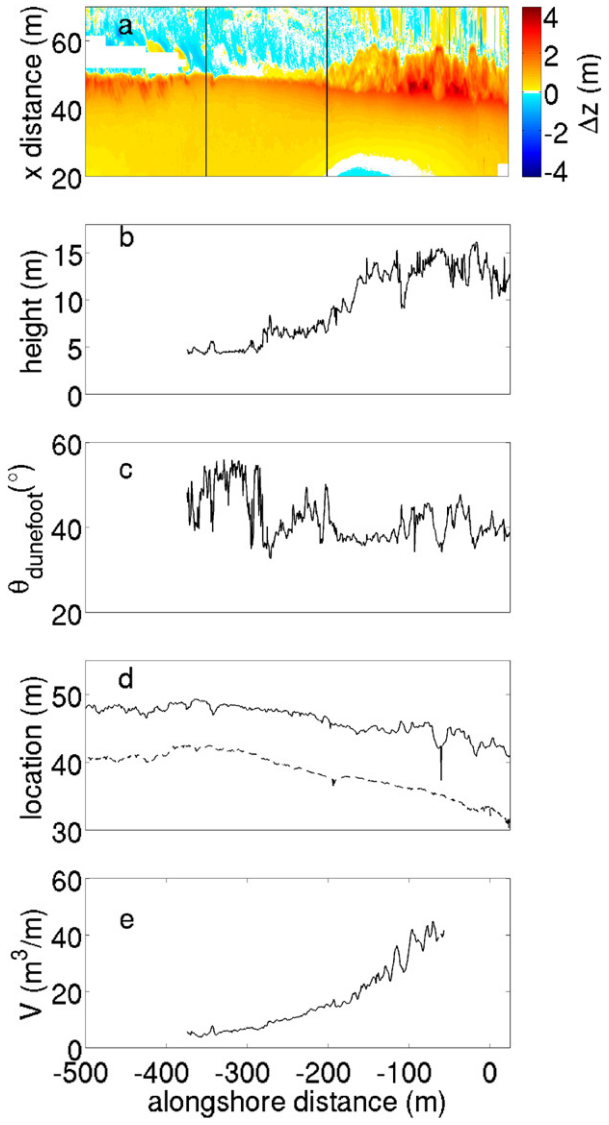


**Fig. 5.** a. Observed bed level change (m); positive represents erosion, negative represents sedimentation; the black lines represent the borders between the different erosion zones discussed in the text, b. height with respect to MSL to which the dune face was affected, c. Slope of eroded part of dune face $\theta_{\text{dunefoot}}$ (°). d. cross-shore location of dune foot, dashed pre-storm, solid post-storm, e. dune erosion volume $V$ ($m^3/m$). In panels b, c and e data are missing as a result of shadowing by the embryo dune field. $V$ could also not be calculated south of $y = -50$ m, due to missing TLS data.

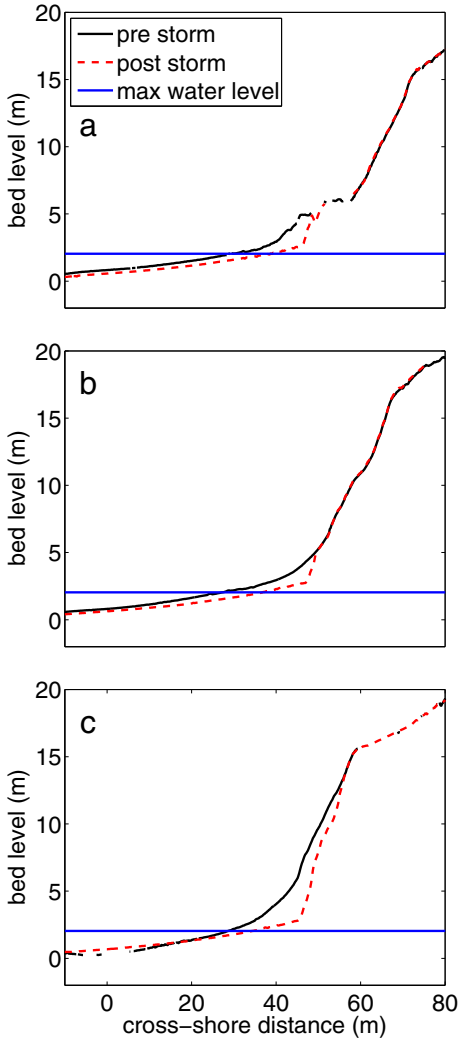


**Fig. 6.** Pre- and post-storm profiles at a. $y = -425$ m, b. $y = -350$ m and c. $y = -80$ m. The maximum offshore water level is depicted in blue.

which in empirical equilibrium dune erosion models (e.g. Van Gent et al., 2008) is taken as the slope transition. The new dune face between the slope break and the maximum erosion height is approximately linear with a slope $\theta_{\text{duneface}}$ near 40° to 50° (≈ 1 : 1, see Fig. 5c). In this study a dune foot height of 3 m is, however, used to be consistent with previous studies along the Dutch coast (e.g. Ruessink et al., 2002; Keijsers et al., 2014) and the definition of a clear bending point in the mild sloping pre-storm dune profile (Fig. 6) is not possible. Along our entire study site the dune foot retreated 5 to 10 m during the storm (Fig. 5d). The dune erosion volume ($V$) per unit alongshore distance, defined here as the volume eroded landward of the pre-storm dune foot, increased from less than 5 $m^3/m$ where the scarp was smallest to some 40 $m^3/m$ in the slump area (Fig. 5e).

### 3.2. Model set-up and morphological calibration

To explore the capabilities of XBeach in hindcasting the observed dune erosion (and alongshore variability therein), we ran XBeach with time-varying wave and water level forcing for the duration of the entire storm, from January 3, 06:00 h to January 6, 09:00 h (Fig. 2). The pre-storm dune and beach topography was used as the initial topography, extended in the seaward direction using the bathymetry surveyed in November 2011. The alongshore model domain was extended by 1.5 km both to the south and the north; here the morphology was taken as alongshore uniform and equaled the morphology at the southern and northern edge of the pre-storm survey area, respectively. The grid resolution in cross-shore direction is 1 m and in the alongshore direction 5 m in the center of our study area, toward the seaward and lateral boundaries $\Delta x$ and $\Delta y$ coarsen to 8 m and 15 m, respectively. Bed level data was written to file every 12.5 h at low tide, allowing us to analyze the bed level change after each high tide (see Fig. 2). The settings in the wave module were $\gamma = 0.55$ and, based on our hydrodynamic calibration of XBeach (Section 2.3). A spin-up time of 30 min was applied, during which the bed level remained unchanged.

The magnitude of $V$ is controlled by the dimensionless parameter 'depth scale' $DS$, which controls several morphological parameters simultaneously that all relate to the avalanching algorithm (threshold depth $eps$, threshold water depth for undertow $h_{\text{min}}$, maximum dune face erosion rate $d_{z\text{max}}$ and water depth at which the algorithm switches from a critical wet slope to a critical dry bed slope $h_{\text{switch}}$, see among others Van Thiel de Vries (2009) and Splinter & Palmsten (2012). Originally, $DS$ was introduced as a scaling parameter between flume

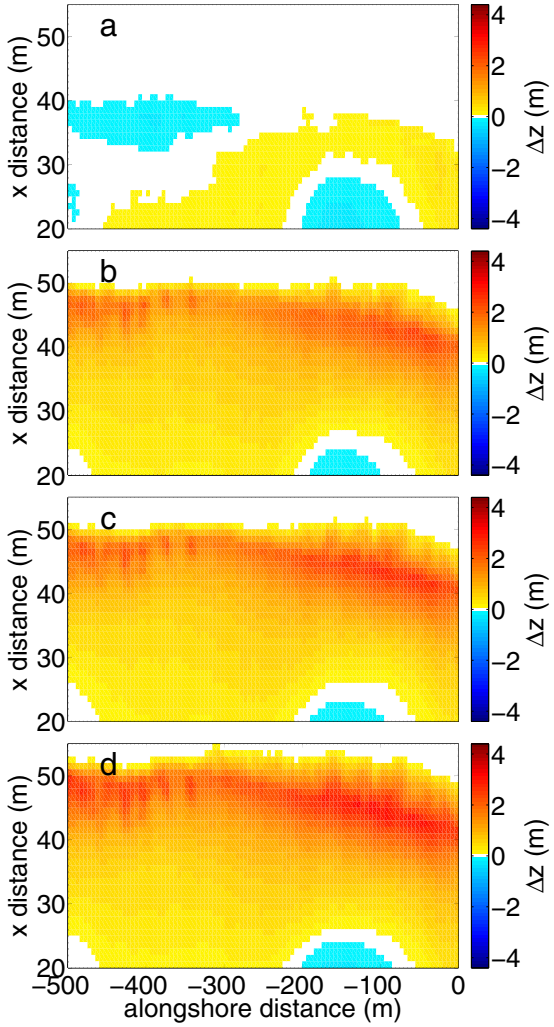


**Fig. 7.** Predicted bed level change (m), with positive values representing erosion a. depth scale $DS = 0.17$, b. $DS = 0.5$, c. $DS = 0.67$, d. $DS = 1$. Note that the panels cover the upper beach and the dune face only. The eroded sand is deposited at $x < 20$ m.

experiments and field cases. In practice, however, $DS$ is a free model parameter to minimize the difference between observed and modeled $V$. To calibrate our morphological settings, we ran 4 simulations with $DS = 0.17$, 0.5, 0.67 and 1. To quantify data-model agreement, we performed an analysis on the observed and modeled bed level change ($\Delta z$) in the area bounded by $y = -500$ to 25 m and $x = 20$ to 55 m. To this end, the modeled topography at the end of the XBeach simulation was interpolated on the post-storm survey grid. The observed and modeled $\Delta z$ were plotted against each other to obtain insight in which bed level changes are modeled correctly (Fig. 8). For this bounded area also a linear regression was performed. Of particular interest are the squared correlation coefficient $r^2$ and the slope $m$ of the regression line; in case of perfect data-model agreement, $r^2 = 1$ and $m = 1$.

With $DS = 0.17$, XBeach produced hardly any dune erosion at all (Fig. 7a), resulting in $r^2 \approx 0$ and $m \approx 0$ (Table 1). The remaining simulations do show erosion (Fig. 7b–d), with surprisingly similar error statistics ($r^2 \approx 0.5$ and $m \approx 0.7$, Table 1). The simulations can be distinguished better when comparing alongshore variations in observed and modeled $V$. For $DS = 0.17$, $V$ is almost 0 in the entire study area, while the other 3 simulations produce alongshore variation pattern in $V$ that is similar to the observed variation pattern (Fig. 9). However, $V$ is underestimated in the area where the slumping extended to 15 m above MSL ($y \approx -100$ m) and overestimated in the area with the dune scarp. With $DS = 0.5$, XBeach does not capture the observed $\Delta z$ around $\Delta z = 1$ m (Fig. 8b red blob at observed $\Delta z = 1$ m and modeled $\Delta z = 0$ m). With $DS = 1$, the model produces numerous bed level changes that were not seen in the observations (Fig. 8d, vertical band at observed $\Delta z = 0$ m). $DS = 0.67$ has less of both mismatches and the erosion of observations versus modeled are closer to the 1:1-line compared to $DS = 0.5$ and $DS = 1$ (Fig. 8c). Based on the linear regression of observed and modeled bed level change and the representation of the three different erosion zones, we consider $DS = 0.67$ as the most accurate setting, while acknowledging that the alongshore variability in erosion volume is underestimated.

### 3.3. Alongshore variation in dune erosion

We designed three additional simulations to explore the reasons for the alongshore variability in $V$. In the first run, termed ALL_UNI, the morphology is entirely alongshore uniform. In the second run, called BATHY_UNI, the measured (and thus alongshore variable) dune profiles were used, but the intertidal and subtidal bathymetry was made alongshore uniform. In the third run, DUNE_UNI, the initial bathymetry comprised the measured intertidal and subtidal bathymetry, but an alongshore uniform dune profile. The profiles were made uniform for $x < 20$ m (approximately $z < 1.5$ m) for BATHY_UNI and $x > 40$ m (approximately $z > 3$ m) for the DUNE_UNI. Between $x = 20$ and $x = 40$ m the profile was re-interpolated to connect smoothly with the original topography. The areas are chosen such that in the simulation that studies the contribution of the dune topography (BATHY_UNI) the full original dune topography is taken into account and that for the simulation where the contribution of the bathymetry is studied (DUNE_UNI), the topography of the intertidal area and deeper varies in longshore direction. With the BATHY_UNI and DUNE_UNI runs, we test whether the alongshore variability in $V$ is induced by alongshore variability in the dune profile (as suggested by Den Heijer, 2013; Van Thiel De Vries et al., 2011) or in the seaward bathymetry (as suggested by Claudino-Sales et al., 2008; Houser et al., 2008, and others), respectively. The study by Van Thiel De Vries et al. (2011) is a theoretical example of dunes with a similar height as Egmond, whereas Claudino-Sales et al. (2008) described the alongshore variation in storm response for Santa Rosa Island after hurricane Ivan, a coast line with typically lower dunes compared to the Dutch coast were part of the dunes were locally inundated during the storm impact. The ALL_UNI run is a reference run to see whether dune erosion is alongshore uniform in case of uniformity in the entire bathymetry; dune erosion may still be somewhat alongshore variable, because of the imposed directional spreading of the short waves and the associated short-crestedness of the incident wave groups. In all three runs, the uniform part of the profile was set equal to that measured in the cross-shore profile at $y = -53$ m, where the observed $V$ was largest (Fig. 5e).

In the ALL_UNI run, both the bed level change and $V$ were essentially constant in the alongshore direction (Figs. 10a and 11). $V$ is now approximately equal to $V$ at $y = -53$ m in the original run. The bed level change and erosion volumes of the BATHY_UNI run with a uniform intertidal and subtidal bathymetry and the measured dune topography resembles the predictions in the simulation with the measured topography closely in all three erosion regions (Figs. 10b and 11). Alongshore variation was also predicted in the DUNE_UNI run (Figs. 10c and 11), but substantially less than in the simulations with the original topography and BATHY_UNI. On the whole, these simulations suggest that the measured alongshore variation in dune erosion was primarily due to alongshore variation in dune topography, with variation in the intertidal and subtidal bathymetry playing a secondary role.

To explore this suggestion further, we examined the temporal evolution of the predicted dune erosion. Fig. 12 shows $V$ after each of the six high tides. Interestingly, the DUNE_UNI run produced some dune erosion around $y = -190$ m after the second high tide, in contrast to the BATHY_UNI run. Apparently, early in the storm, the bathymetry governs the alongshore variability in dune erosion. The pre-storm

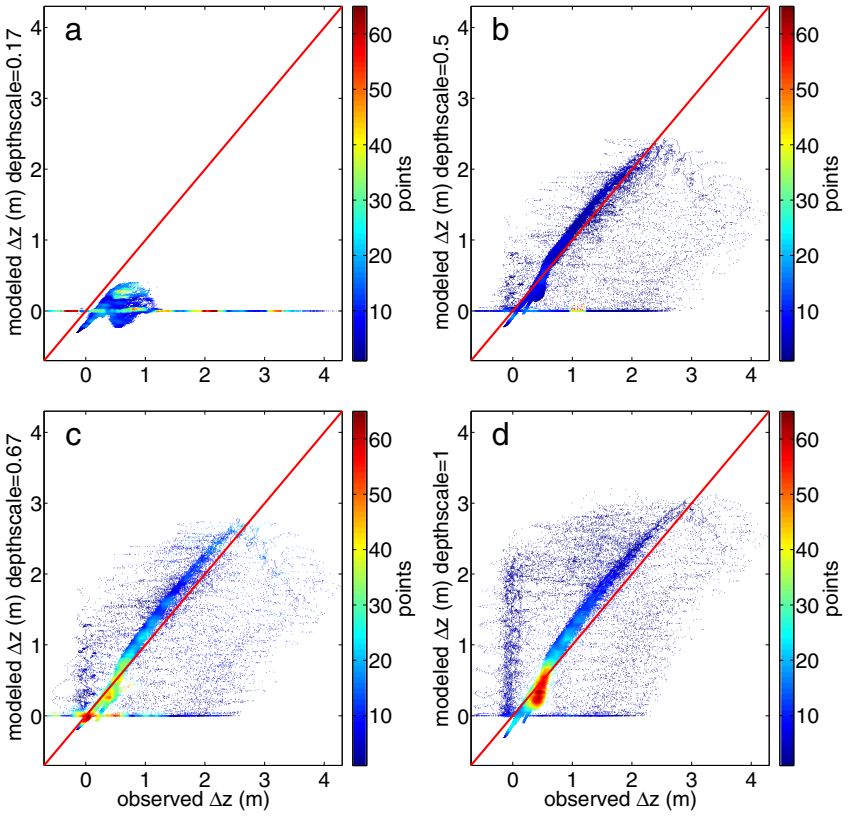


**Fig. 8.** Bed level change $\Delta z$ (m) for depthschale $DS = 0.17$, 0.5, 0.67 and 1. Erosion is defined as positive, therefore in this figure, positive values represent a decrease in $\Delta z$.

intertidal sand bar at $y = -190$ m was less well developed than elsewhere (Fig. 13). In the DUNE_UNI run the depression in the sandbar caused the waves to just reach the dune foot, resulting in localized erosion. The BATHY_UNI run contained the more well-developed intertidal sand bar from $y = -53$ m in the entire domain, and the dunes did not erode. The alongshore variability in the BATHY_UNI run arose primarily during the fifth and sixth high tides, when the dune erosion was observed to be most severe. With the substantial higher surge levels, dune erosion was predicted along the entire model domain, with its magnitude governed by characteristics of the dune profile. Clearly, the pre-storm embryo dune field ($y = -500$ to $-350$ m) eroded. Elsewhere, the type (and magnitude) of erosion appears to be governed largely by the steepness of the dune face. In the region where the scarp developed ($y = -350$ to $-200$ m), the contour lines around the maximum surge level are farther apart than in the region with slumps $y = -200$ to 0 m (Fig. 13a). Probably, it took most of the fifth and sixth high tides to erode this relatively large volume of sand in the lower part of the dune at the location with the relatively less steep lower dune face, and the dune face higher up remained unaffected. In a way, these results are analogous to XBeach model results in Van Thiel De Vries et al. (2011), who found that for the same wave forcing a higher dune resulted in a larger $V$ because more sand will collapse onto the beach. In the case of the erosion at Egmond during the January 2012 storm, the dune height is approximately alongshore uniform. There is, however, variation in the steepness of the lower part of the dune (Fig. 13c). This variation in steepness determines the availability of sand around the maximum storm surge level. In the area with a steeper dune front ($y = -200$ to 0 m) more slumping occurred and more sand collapsed on the beach. During the fifth and sixth high tides large offshore angles of incidence were measured (Fig. 3). This could have resulted in strong alongshore currents that may have redistributed the sand after slumping, hence removing this potential sand buffer and leading to large erosion volumes at the area with a steep profile around the maximum storm surge level. It is possible that a substantially stronger storm, in particular with a higher surge level, would have caused less alongshore variability in $V$ than observed now. XBeach simulations in De Winter (2014) confirm this suggestion.

**Table 1**
Results of linear regression analysis of the observed and predicted topographic change in the area bounded by $y = -500$ to 25 m and $x = 20$ to 55 m; $r^2$ is the squared correlation coefficient, $m$ is the slope of the regression line.

| depth scale | $r^2$ | $m \pm 95$ % range |
|---|---|---|
| .17 | 0 | $0 \pm 0.0012$ |
| .50 | 0.48 | $0.60 \pm 0.0046$ |
| .67 | 0.55 | $0.72 \pm 0.0049$ |
| | 0.50 | $0.81 \pm 0.0060$ |

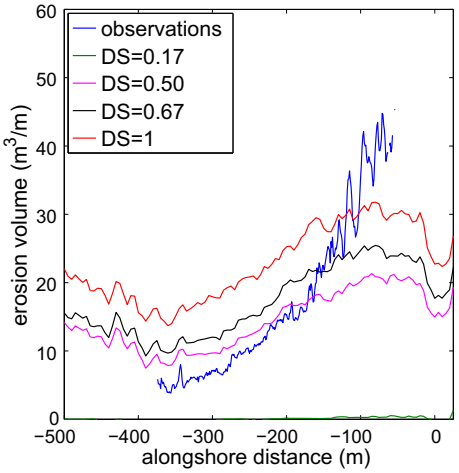


**Fig. 9.** Erosion volume $V$ (m$^3$/m) versus alongshore distance for different depth scale $DS$.

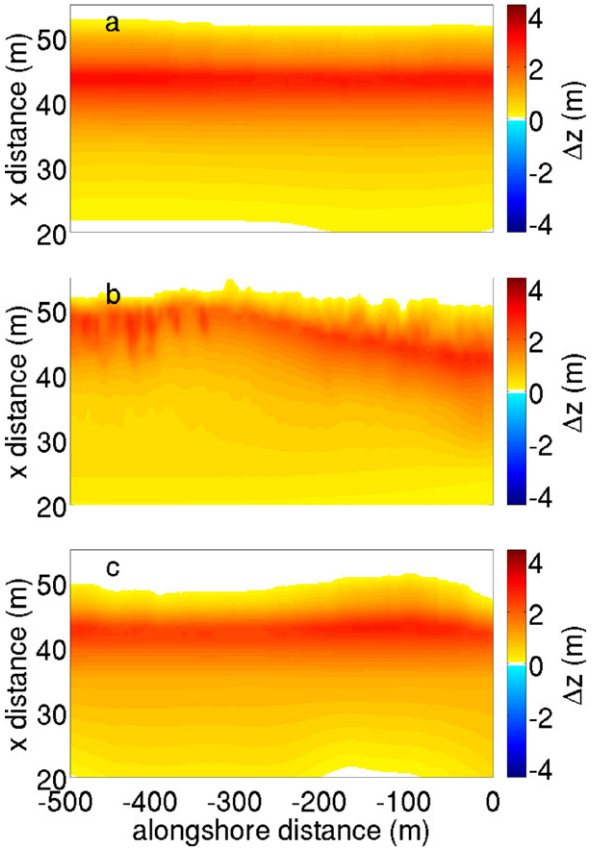


**Fig. 10.** Predicted bed level change (m), with positive values representing erosion for the a. ALL_UNI, b. BATHY_UNI and c. DUNE_UNI runs.

## 4. Discussion

The storm we analyzed eroded between 5 and 40 $m^3/m$ in a few hours. This is in the same range as what is added by aeolian processes during one or more years as measured by annual surveys (e.g. De Vries et al., 2012) and depicted in Fig. 1. The erosion volumes discussed in this paper are in the same order of magnitude of previous observations of *V*. Previous storms at the Dutch coast showed *V*, with 80 to 100 $m^3/m$ for a major storm in 1953, 15 to 80 $m^3/m$ in 1976 and 2 to 55 $m^3/m$ in 1983 (De Vries et al., 2012). However, according to Dutch coastal policy, the dune at Egmond should be able to withstand

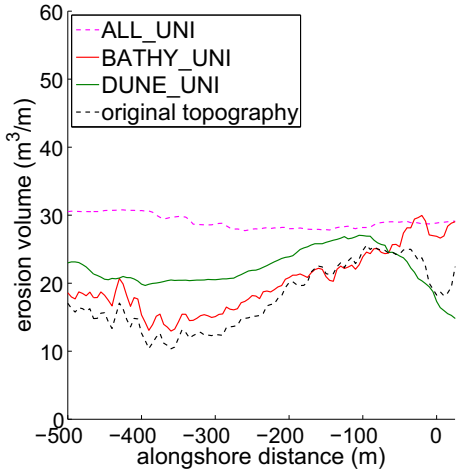


**Fig. 11.** Observed and predicted erosion volume *V* ($m^3/m$) versus alongshore distance, for different model simulations.

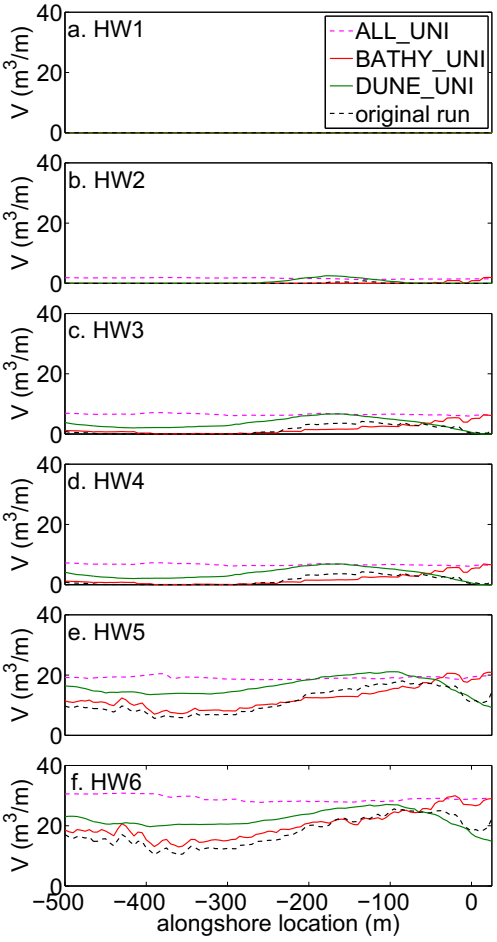


**Fig. 12.** Predicted dune erosion volume *V* ($m^3/m$) for different simulations, after each high water, see Fig. 2c, versus alongshore distance (m).

a storm with a return frequency of 1:10,000 year. It is expected that for these storms *V* is approximately 300 $m^3/m$ to 600 $m^3/m$ (Vellinga, 1986).

We were able to validate the hydrodynamical setting of our 2D-XBeach model and concluded that the default setting for *n* and γ results in optimum agreement when both $H_{ss}$ and $H_{inf}$ are considered simultaneously. The morphological development in XBeach required tuning of *DS*, which influences several other parameters. Because these parameters are changed simultaneously, the individual effect of a parameter on *V* is difficult to elucidate. Originally, *DS* was introduced as a scaling parameter, with a default value for field cases of $DS = 0.17$. This value, however, did not produce any dune erosion for the storm considered here. Ideally, *DS* should be replaced by a more physics based predictor for dune scarping and slumping.

## 5. Conclusion

The significant height of short and infragravity waves in the intertidal zone is reproduced most accurately using the default settings of XBeach, with a root–mean–square error of 0.086 and 0.043 m for the short and infragravity wave height in our data set. The error for the short waves can be reduced with other values of the free parameters; however, this goes at the expense of an increasing error in the infragravity wave height, presumably because the grouped structure of the short waves is affected adversely.

When tuned, XBeach predicts the magnitude and pattern of alongshore variations in erosion volume reasonably well for the January 2012 storm at Egmond. In more detail, XBeach over predicts erosion volume

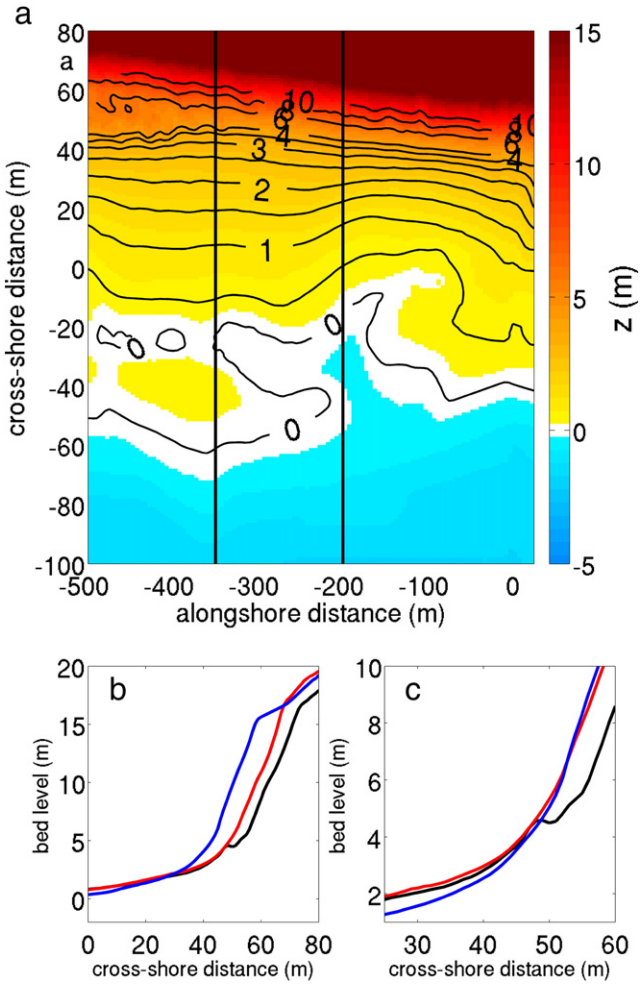


**Fig. 13.** a. Pre-storm model bathymetry, with contour lines. In the northern part ($y = -400$ to $-300$ m) the contour lines are further apart than at the southern part (around $y = -80$ m) where the dune face slumped. b. Cross-section of the middle of each zone, black $y = -424$ m, red $y = -350$ m, blue $y = -80$ m. c close up of the same area, the profile of $y = -80$ m is shifted landward, so the steepness of the cross-sections can be compared better.

in the region where a dune scarp developed and underestimated the erosion volume where the whole dune face collapsed in a series of slumps. For our study side additional XBeach simulations illustrate that the observed alongshore variation in erosion volume is steered primarily by the pre-storm dune topography (i.e., presence of embryo dune field and the steepness of the dune front). The importance of alongshore variability in intertidal beach topography is secondary, but not negligible during the initial stage of the storm, when the surge level was still low.

## Acknowledgments

RCdW and BGR acknowledge funding by the Utrecht University's focus area “Earth and Sustainability”, sub-theme “Earth and Climate”.

## References

Bender, C.J., Dean, R.G., 2003. Wave field modification by bathymetric anomalies and resulting shoreline changes: a review with recent results. Coast. Eng. 49, 125–153.
Callaghan, D.P., Ranasinghe, R., Roelvink, J.A., 2013. Probabilistic estimation of storm erosion using analytical, semi-empirical, and process based storm erosion models. Coast. Eng. 82, 64–75.
Claudino-Sales, V., Wang, P., Horwitz, M.H., 2008. Factors controlling the survival of coastal dunes during multiple hurricane impacts in 2004 and 2005: Santa Rosa barrier island, Florida. Geomorphology 95, 295–315.
Corbella, S., Stretch, D.D., 2012. Predicting coastal erosion trends using non-stationary statistics and process-based models. Coast. Eng. 70, 40–49.
De Bakker, A.T.M., Tissier, M.F.S., Ruessink, B.G., 2014. Shoreline dissipation of infragravity waves. Cont. Shelf Res. 72, 73–82.
De Vries, S., Southgate, H.N., Kanning, W., Ranasinghe, R., 2012. Dune behavior and aeolian transport on decadal timescales. Coast. Eng. 67, 41–53.
De Winter, R.C., 2014. Dune Erosion Under Climate Change. (Ph.D. thesis). Utrecht University.
Den Heijer, C., 2013. The Role of Bathymetry, Wave Obliquity and Coastal Curvature in Dune Erosion Prediction. (Ph.D. thesis). Delft University of Technology, Deltares.
Den Heijer, C., Baart, F., van Koningsveld, M., 2012. Assessment of dune failure along the Dutch coast using a fully probabilistic approach. Geomorphology 143–144 (95â€“103.).
Galal, E.M., Takewaka, S., 2011. The influence of alongshore and cross-shore wave energy flux on large- and small-scale coastal erosion patterns. Earth Surf. Process. Landf. 36, 953–966.
Gongriep, F., 2013. Observations and Modeling of Alongshore Variation in Dune Erosion. (Master's thesis). Utrecht University.
Houser, C., Hapke, C., Hamilton, S., 2008. Controls on coastal dune morphology, shoreline erosion and barrier island response to extreme storms. Geomorphology 100, 223–240.
Keijsers, J.G.S., Poortinga, A., Riksen, M.J.P.M., Maroulis, J., 2014. Spatio-temporal variability in accretion and erosion of coastal foredunes in the Netherlands: regional climate and local topography. PLoS ONE 9, e91115.
Kobayashi, N., Buck, M., Payo, A., Johnson, B., 2009. Berm and dune erosion during a storm. J. Waterw. Port Coast. Ocean Eng. 135, 1–10.
Kriebel, D.L., Dean, R.G., 1993. Convolution method for time-dependent beach-profile response. J. Waterw. Port Coast. Ocean Div. ASCE 119, 204–226.
Larson, M., Erikson, L., Hanson, H., 2004. An analytical model to predict dune erosion due to wave impact. Coast. Eng. 51, 675–696.
Long, J.W., De Bakker, A.T.M., Plant, N.G., 2014. Scaling coastal dune elevation changes across storm-impact regimes. Geophys. Res. Lett. 41, 2899–2906.
Masselink, G., Kroon, A., Davidson-Arnott, R.G.D., 2006. Morphodynamics of intertidal bars in wave-dominated coastal settings — a review. Geomorphology 73, 33–49.
McCall, R., Van Thiel de Vries, J.S.M., Plant, N.G., Van Dongeren, A.R., Roelvink, J.A., Thompson, D.M., Reniers, A.J.H.M., 2010. Two-dimensional time dependent hurricane overwash and erosion modeling at Santa Rosa Island. Coast. Eng. 57, 668–683.
Palmsten, M.L., Holman, R.A., 2011. Infiltration and instability in dune erosion. J. Geophys. Res. Oceans 116, C10030.
Pape, L., Plant, N.G., Ruessink, B.G., 2010. On cross-shore migration and equilibrium states of nearshore sandbars. J. Geophys. Res. 115.
Quartel, S., Ruessink, B.G., Kroon, A., 2007. Daily to seasonal cross-shore behaviour of quasi-persistent intertidal beach morphology. Earth Surf. Process. Landf. 32, 1293–1307.
Roelvink, J.A., 1993. Dissipation in random wave groups incident on a beach. Coast. Eng. 19, 127–150.
Roelvink, D., Reniers, A., van Dongeren, A., van Thiel de Vries, J., McCall, R., Lescinski, J., 2009. Modelling storm impacts on beaches, dunes and barrier islands. Coast. Eng. 56, 1133–1152.
Ruessink, B.G., Jeuken, M.C.J.L., 2002. Dunefoot dynamics along the Dutch coast. Earth Surface Processes and Landforms. 27 pp. 1043–1056.
Russell, P., 1993. Mechanisms for beach erosion during storm. Cont. Shelf Res. 13, 1243–1265.
Schupp, C.A., McNinch, J.E., List, J.H., 2006. Nearshore shore-oblique bars, gravel outcrops, and their correlation to shoreline change. Mar. Geol. 233, 63–79.
Splinter, K.D., Palmsten, M.L., 2012. Modeling dune response to an east coast low. Mar. Geol. 329–331, 46–57.
Splinter, K.D., Carley, J.T., Golshani, A., Tomlinson, R., 2014. A relationship to describe the cumulative impact of storm clusters on beach erosion. Coast. Eng. 83, 49–55.
Stockdon, H.F., Thompson, D.M., Plant, N.G., Long, J.W., 2014. Evaluation of wave runup predictions from numerical and parametric models. Coast. Eng. 92, 1–11.
Thornton, E.B., MacMahan, J., Sallenger Jr., A.H., 2007. Rip currents, mega-cusps, and eroding dunes. Mar. Geol. 240, 151–167.
Van de Graaff, J., 1977. Dune erosion during a storm. Coast. Eng. 1, 99–134.
Van Enckevort, I.M.J., Ruessink, B.G., 2001. Effects of hydrodynamics and bathymetry on video estimates of nearshore sandbar position. J. Geophys. Res. 106, 16969–16979.
Van Gent, M.R.A., van Thiel de Vries, J.S.M., Coeveld, E.M., de Vroeg, J.H., van de Graaff, J., 2008. Large-scale dune erosion tests to study the influence of wave periods. Coast. Eng. 55, 1041–1051.
Van Rijn, L.C., Tonnon, P.K., Sánchez-Arcilla,, A.b., Cáceres,, I.b., Grüne, J., 2011. Scaling laws for beach and dune erosion processes. Coast. Eng. 58, 623–636.
Van Thiel de Vries, J.S.M., 2009. Dune Erosion During Storm Surges. (Ph.D. thesis). Delft University of Technology.
Van Thiel de Vries, J.S.M., van Gent, M.R.A., Walstra, D.J.R., Reniers, A.J.H.M., 2008. Analysis of dune erosion processes in large-scale flume experiments. Coast. Eng. 55, 1028–1040.
Van Thiel De Vries, J., Dongeren, A.V., McCall, R., Reniers, A., 2011. The effect of the longshore dimension on dune erosion. 32nd International Conference on Coastal Engineering. ICCE 2010, June 30–July 5 2010, Shanghai, China.
Vellinga, P., 1982. Beach and dune erosion during storm surges. Coast. Eng. 6, 361–387.
Vellinga, P., 1986. Beach and Dune Erosion During Storm Surges. (Ph.D. thesis). Delft University.